CORE
Metadata, citation and similar papers at core.ac.uk
Provided by Bilkent University Institutional Repository

Available online at www.sciencedirect.com
ScienceDirect
Current Applied Physics 9 (2009) 472–477
Current Applied Physics
An official journal of the K@S
www.elsevier.com/locate/cap
www.kps.or.kr

The effect of Si_xN_y interlayer on the quality of GaN epitaxial layers grown on Si(1 1 1) substrates by MOCVD

Engin Arslan [a,*], Mustafa K. Ozturk [b], Suleyman Ozcelik [b], Ekmel Ozbay [a]

[a] *Nanotechnology Research Center-NANOTAM, Department of Physics, Department of Electrical and Electronics Engineering, Bilkent University, 06800 Ankara, Turkey*
[b] *Department of Physics, Faculty of Science and Arts, Gazi University, Teknikokullar, 06500 Ankara, Turkey*

Received 8 January 2008; received in revised form 10 April 2008; accepted 10 April 2008
Available online 27 April 2008

Abstract

In the present paper, the effects of nitridation on the quality of GaN epitaxial films grown on Si(1 1 1) substrates by metal–organic chemical vapor phase deposition (MOCVD) are discussed. A series of GaN layers were grown on Si(1 1 1) under various conditions and characterized by Nomarski microscopy (NM), atomic force microscopy (AFM), high resolution X-ray diffraction (HRXRD), and room temperature (RT) photoluminescence (PL) measurements. Firstly, we optimized LT-AlN/HT-AlN/Si(1 1 1) templates and graded AlGaN intermediate layers thicknesses. In order to prevent stress relaxation, step-graded AlGaN layers were introduced along with a crack-free GaN layer of thickness exceeding 2.2 μm. Secondly, the effect of in situ substrate nitridation and the insertion of an Si_xN_y intermediate layer on the GaN crystalline quality was investigated. Our measurements show that the nitridation position greatly influences the surface morphology and PL and XRD spectra of GaN grown atop the Si_xN_y layer. The X-ray diffraction and PL measurements results confirmed that the single-crystalline wurtzite GaN was successfully grown in samples A (without Si_xN_y layer) and B (with Si_xN_y layer on Si(1 1 1)). The resulting GaN film surfaces were flat, mirror-like, and crack-free. The full-width-at-half maximum (FWHM) of the X-ray rocking curve for (0 0 0 2) diffraction from the GaN epilayer of the sample B in ω-scan was 492 arcsec. The PL spectrum at room temperature showed that the GaN epilayer had a light emission at a wavelength of 365 nm with a FWHM of 6.6 nm (33.2 meV). In sample B, the insertion of a Si_xN_y intermediate layer significantly improved the optical and structural properties. In sample C (with Si_xN_y layer on $Al_{0.11}Ga_{0.89}N$ interlayer). The in situ depositing of the, however, we did not obtain any improvements in the optical or structural properties.
© 2008 Elsevier B.V. All rights reserved.

PACS: 61.10.Nz; 68.37.Ps; 72.80.Ey; 78.55.Cr

Keywords: B1. GaN; B1. AlN layer; B1. Step graded AlGaN; A3. MOCVD; B1. Silicon substrates; B1. Intermediate layer

1. Introduction

As a substrate for the growth of GaN/AlGaN epitaxial layers, silicon has many advantages compared to SiC and sapphire due to its high crystal quality, low cost, good electrical and thermal conductivity, and large-area size [1–8]. Due to these advantages, gallium nitride growth on Si(1 1 1) wafers has attracted considerable academic and commercial attention. However, because of the large mismatches in the lattice parameters (−16.9%) and thermal expansion coefficients (approximately 113%) between Si and GaN, it is rather difficult to epitaxially grow GaN on Si substrates [9–15]. Due to large lattice mismatch a high density of threading dislocations on the order of ($10^9 \sim 10^{10}$ cm^{-2}) exists in the GaN film on silicon substrates, which significantly affects the performance of the GaN based devices [2]. On the other hand, cracks are typically formed either due to the large tensile stress in the GaN film during growth or during the cooling down

* Corresponding author. Tel.: +90 312 2901019; fax: +90 312 2901015.
E-mail address: engina@bilkent.edu.tr (E. Arslan).

1567-1739/$ - see front matter © 2008 Elsevier B.V. All rights reserved.
doi:10.1016/j.cap.2008.04.008

process with large differences in the thermal expansion coefficient between GaN and Si [9–15]. The growth conditions and quality of the crystals strongly affect the crack density. The average size of the crack-free surface areas on an epitaxial sample can be increased by manipulating the growth conditions as well as the post-growth heat treatment. However, the appearance of the cracks is quite random on the film, which produces a fatal difficulty in device applications. Therefore, the control of crack distribution for a large-area film is the main issue of the present study [8–11].

Many methods have been reported to eliminate the cracks and to improve crystal quality. Min-Ho Kim et al. [13] used a five-step graded $Al_xGa_{1-x}N$ ($x = 0.87-0.07$) interlayer between AlN buffer layer and GaN on Si(1 1 1). An AlGaN/GaN superlattice was used by Nikishin et al. [9] instead of an AlGaN layer. The insertion of a low temperature AlN (LT-AlN) interlayer into the bulk high growth temperature GaN, which was proposed by Amano et al. [10]. Graded AlGaN intermediate layers between the AlN nucleation layer (NL) and GaN introduces compressive stress during growth in order to compensate for the tensile stress that is generated primarily during the cool down from the growth temperature [14].

However, because of the excessively large thermal expansion coefficient mismatch, these methods have not achieved perfect GaN/Si(1 1 1) epitaxy when compared with the growth of GaN on sapphire substrate [4,5].

It has been recently demonstrated that defect-free GaN on Si was present when an Si_xN_y buffer was used for the GaN grown by MOCVD [16] and by hot wall chemical vapor deposition [17]. This buffer was achieved by nitridating the Si substrate with N_2 flow at at 900 °C by Uena et al. [16] and at 1120 °C by Huang et al. [17]. Additionally, a double-buffer structure of AlN/Si_xN_y was used by molecular beam epitaxy [18] where single-crystalline Si_xN_y was obtained by introducing the active nitrogen plasma to the Si(1 1 1) surface at 900 °C for approximately 30 s. Hageman et al. [19] showed the insertion of an Si_xN_y intermediate layer on a 1 μm GaN layer significant improves the optical and structural properties of the GaN layer.

In the present paper, we demonstrate the extremely smooth and flat GaN high-quality and nearly crack-free GaN/Si(1 1 1) epitaxy. We investigated the effect of in situ substrate nitridation and the insertion of an Si_xN_y mask interlayer on the GaN crystalline quality in the Si(1 1 1)/30 nm HT-AlN/30 nm LT-AlN/400 nm HT-AlN/$Al_xGa_{1-x}N$/GaN sample structures. The epitaxial quality of the GaN film significantly improved by the Si_xN_y layer grown on Si(1 1 1) substrate.

2. Experimental procedure

GaN epitaxial layers on Si-substrate were grown in a low-pressure MOCVD reactor (Aixtron 200/4 HT-S), using Trimethylgallium (TMGa), trimethylaluminum (TMAl), and ammonia as Ga, Al and N precursors, respectively. The H_2 was used as a carrier gas during AlN and AlGaN growth. Before loading the substrates, Si substrates were sequentially degreased by H_2OSO_4:H_2O_2:H_2O (2:1:1) solutions for 1 min, and etched in a 2% HF solution for 1 min, rinsed in de-ionized water, and dried with a nitrogen gun.

At the beginning of the growth, the substrate was baked in an H_2 ambient at 1100 °C for 20 min in order to remove the native oxide. Three different samples were grown with an optimized buffer layer. In sample A, to prevent the formation of the amorphous Si_xN_y layer, we carried out 3 s Al pre-deposition on the silicon surface (Fig. 1 a). In samples B and C, we performed nitridation on different layers of the surface (Fig 1b and c). To grow an Si_xN_y mask layer on an Si(1 1 1) substrate surface in sample B, following the thermal etching, the substrate was nitridated by exposing it to the NH_3 flow of 0.90 slm for 10 min at 1020 °C. Nitridation in sample C was performed on the $Al_{0.11}Ga_{0.89}N$ interlayer. The in situ depositing of the Si_xN_y layer took place at 1020 °C with the introduction of silane (150 sccm) to the NH_3 flow (3 slm) for 120 s.

The buffer structures and growth conditions of all the samples were the same and included: low-temperature (700 °C) AlN (LT-AlN) layers, high temperature (1100 °C) AlN (HT-AlN) layers, and seven-step graded $Al_xGa_{1-x}N$ interlayer ($x = 0.74$, 0.64, 0.54, 0.40, 0.33, 0.22, 0.11). In all of the samples, the GaN layers were grown at 1050 °C. The AlN template layer growth temperature produces the best crystalline quality and a reasonably low tensile stress in the layer. The structure of the sample's buffer layer is Si(1 1 1)/30 nm HT-AlN/30 nm LT-AlN/400 nm HT-AlN/$Al_xGa_{1-x}N$/GaN. The AlGaN layer's thickness ratio was approximately: 1:1.5:2:2.5:3:3.5:4. The total thickness of the AlGaN was 750 nm.

The crystalline quality of the GaN layers was examined by high resolution X-ray diffraction (XRD). The X-ray diffraction was performed using a Bruker D8 system, delivering a Cu Kα1 line. The optical properties were investigated by photoluminescence (PL) measurements performed at room temperature. PL spectra were excited using a He–Cd

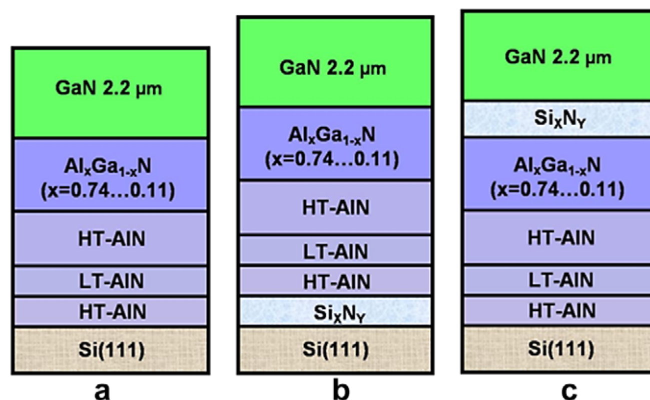

Fig. 1. Schematical view of GaN/Si(1 1 1) with (a) HT-AlN/LT-AlN/HT-AlN/$Al_xGa_{1-x}N$, (b) SiN_x/HT-AlN/LT-AlN/HT-AlN/$Al_xGa_{1-x}N$ and (c) HT-AlN/LT-AlN/HT-AlN/$Al_xGa_{1-x}N$/ SiN_x buffer system.

laser (325 nm) with an excitation power of 15 mW. The surface morphology of the top GaN film was observed by Nomarski interface contrast optical microscopy and atomic force microscope (AFM).

3. Results and discussion

Fig. 2a–c shows the Nomarski microscopy photos of samples A, B, and C. The surface morphologies of all the

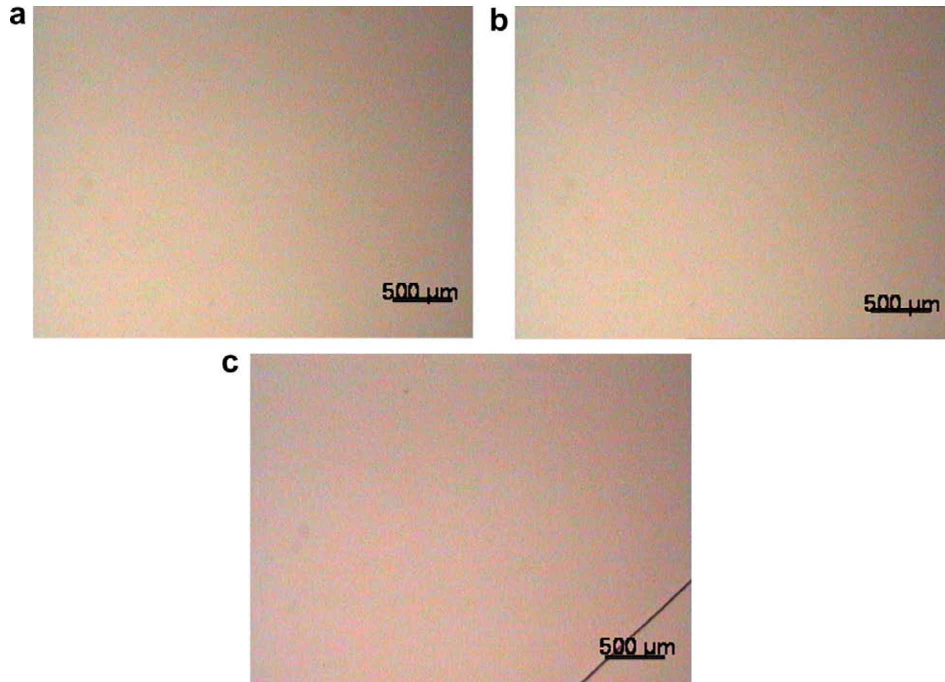

Fig. 2. Optical Nomarski microscopy view of (a) sample A, (b) sample B, and (c) sample C.

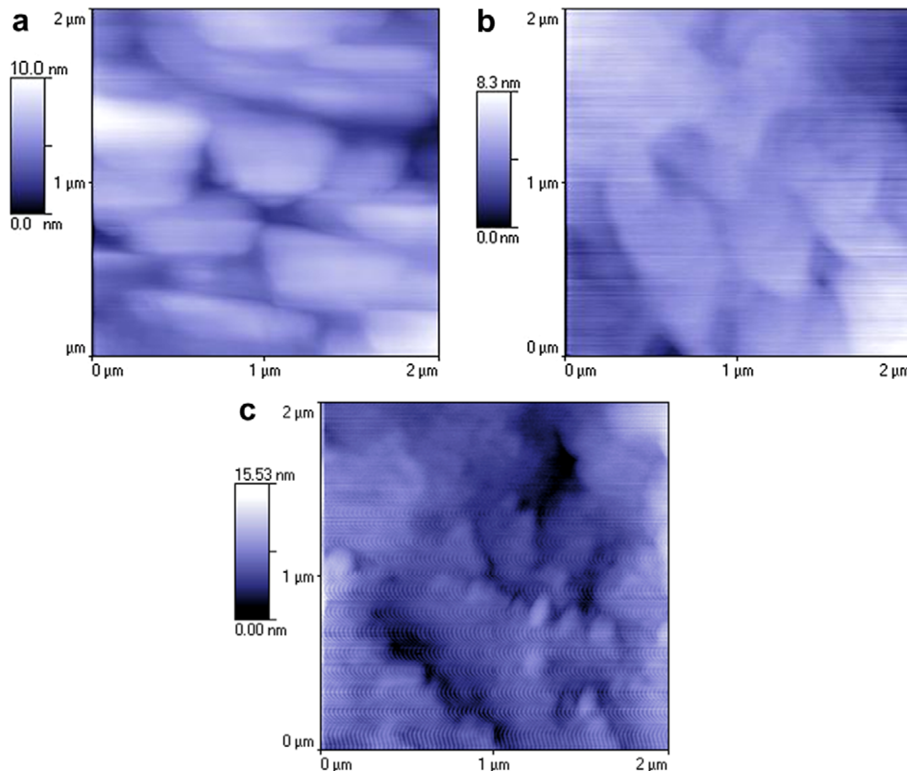

Fig. 3. AFM images of AFM scans (2 µm × 2 µm scans) of GaN films in (a) sample A, (b) sample B, and (c) sample C.

samples were studied by optical Nomarski interference microscopy. The crack density changes with the Si_xN_y interlayer position. In the present paper, we have shown a variation of cracks with the Si_xN_y interlayer. The lowest crack density was achieved on sample B with GaN film grown on nitridated silicon substrates. In sample C, the insertion of a Si_xN_y intermediate layer increased the crack density in the sample. The cracks along the {1−100} in the GaN layers grown on Si substrate have already been reported by many groups [8,13,24,29]. Cracks in the GaN on Si are known to be formed during the cooling stage due to the large tensile stress caused by the large difference in the thermal expansion coefficients [20,22–24].

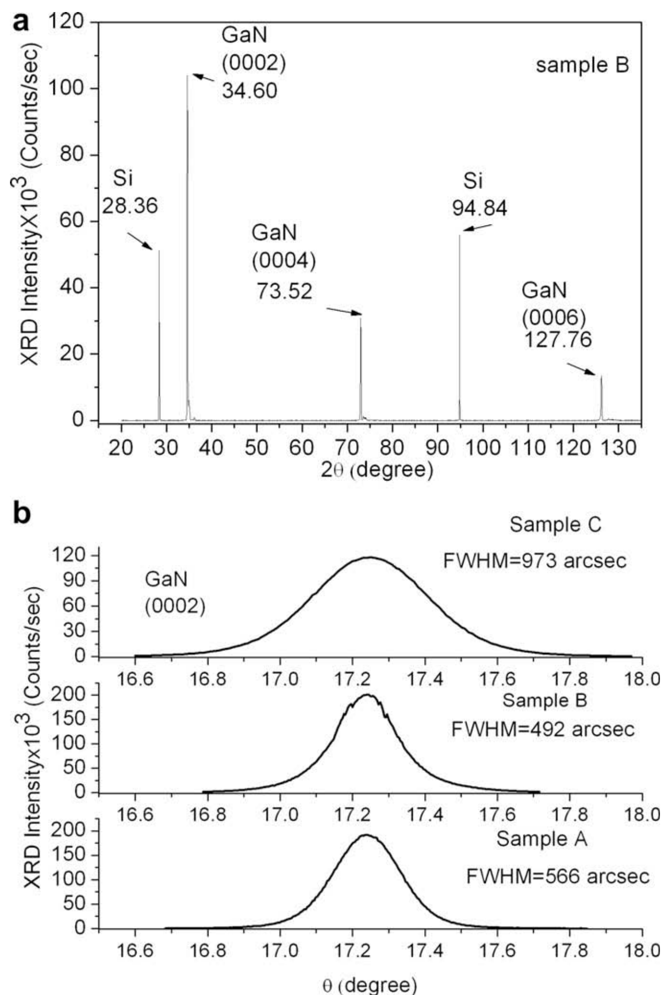

Fig. 4. (a) $\omega-2\theta$ scan X-ray diffraction pattern and (b) θ scan X-ray diffraction pattern of the sample B, and (c) θ-rocking curve of the (0002) reflection of the GaN peak of all the samples.

The surface morphology of the GaN layer grown on nitrided Si substrate is extremely smooth. The root-mean-square (RMS) roughness and the maximum peak-to-valley roughness are between 0.8 nm and 12.3 nm. Fig. 3 shows a comparison of the surface morphology for the samples. Sample B has a smooth surface with low rms roughness (rms = 0.8 nm) compared to sample A (rms = 0.9 nm) and sample C (rms = 12.3 nm). Sample B with nitrided substrate shows fewer defects, but sample C with an Si_xN_y intermediate interlayer on an $Al_{0.11}Ga_{0.89}N$ interlayer shows structural defects along with a rough morphology, in which similar surface defects have been associated with open core dislocations that have a screw-type component [12,20,21].

X-ray diffraction (XRD) was performed for all of the samples to investigate the crystal phase of the GaN on Si(111). Fig. 3a shows a typical $\omega-2\theta$ scan XRD pattern of a GaN layer grown on a 400 nm HT-AlN and 700 nm graded $Al_xGa_{1-x}N$ interlayer, with nitrided Si(111) substrate, in sample B. It exhibited only the dominant wurtzite GaN crystalline (0002), (0004) and (0006) peaks plus two peaks from Si substrate. The (0002), (0004), and (0006) reflections of wurtzite GaN are clearly observed at 34.60°, 73.52°, and 127.76°, respectively. These results indicate a grown GaN layer with the normal orientation along the c-axis of wurtzite crystalline structures [12,26].

Fig. 4b reveals the (θ-rocking curve for GaN (0002) reflection peak for sample B. The FWHMs values of the symmetric (0002) rocking curve, ω-scan as well as the symmetric $\omega-2\theta$ scan, are shown in Table 1. The FWHM of the GaN (0002) peak were in the range of 492–973 arcsec. It is shown that with the Si_xN_y mask on the Si substrate the FWHM of XRD peak decreases from 566 to 492 arcsec, which is indicative of a significant improvement. The results are comparable to the best result of 600 arcsec reported by Armin Dadgar et al. [25]. On the other hand, these values are better than 790–730 arcsec, which were obtained by Cheng et al. [20]. We also obtained rather low FWHM values for the symmetric $\omega-2\theta$ scan of the GaN (0002) peak. We did not obtain, however, an improvement of the material quality with Si_xN_y interlayer on the $Al_{0.11}Ga_{0.89}N$ interlayer.

Table 1
Properties of the GaN layers grown without nitridation and with nitridation on different layers are listed

Sample ID	PL peak position (nm)	FWHM of PL (nm)	FWHM of (0002) ω-scan XRC (arcsec)	FWHM of (0002) $\omega-2\theta$ scan XRC (arcsec)	Rms roughness (nm)
A	365	6.7	588	273	0.9
B	365	6.6	492	254	0.8
C	367	7.2	973	481	12.3

The second and third columns show the peak position and FWHM (nm) of the band emission of PL at room temperature. In the fourth and fifth column, FWHM (arcsec) of ω-scan and $\omega-2\theta$ scan XRC curve for (0002) reflection of GaN, are listed respectively. The last column shows the rms surface roughness (nm) measured for a $2 \times 2\ \mu m^2$ scan area.

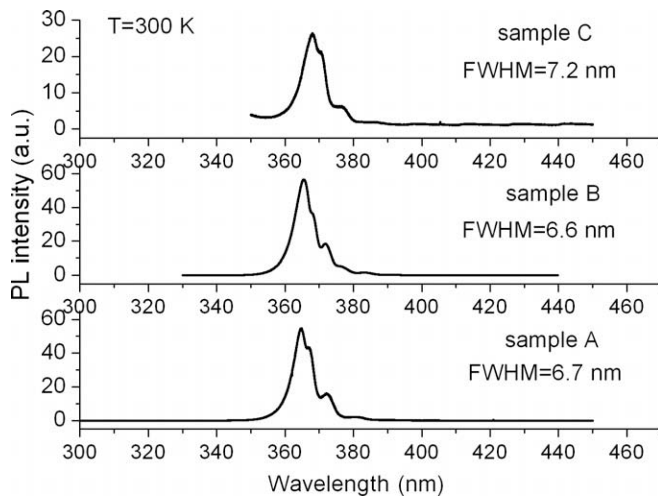

Fig. 5. PL spectra and its FWHMs values recorded at room temperature (RT) for the samples.

The photoluminescence (PL) spectra at room temperature for all of the samples are shown in Fig. 5. The PL peak and FWHM values for the samples are all shown in Table 1. The samples show a strong PL emission band between 365 and 367 nm (3.40–3.38 eV) due to the near band edge emission from wurtzite GaN. In the literature, the PL emission band for the GaN on sapphire substrate is between 361 and 363 nm [30]. The FWHMs of the band edge emission were in the range of 6.6–7.2 nm. The small FWHM values of the PL emission peaks also indicate high-quality w-GaN material. It can be seen in Table 1 and Fig. 5 that there is a red-shifted peak between sample B, and sample C is 2 nm. In our case, this may have been due to the lattice deformation resulting from the difference in the thermal expansion coefficients of GaN and Si [27,28].

Fig. 5 shows the PL spectra taken from the samples. This spectrum shows very low intensity of emission at 373 nm. For sample C, this emission peak intensity was lower than the other samples. We also did not observe its presence in the GaN layers grown on sapphire. Further investigation is needed to clarify its origin.

The blue shift of PL emission energy was considered to be a result induced by the compressive strain in a HT-GaN film on sapphire substrate by Iwaya et al. [31]. Additionally, Tsai et al. [30] found that in GaN film on sapphire substrate, the RT near band edge PL emissions energy are shifted to lower energies, namely, 3.45 and 3.43 eV, respectively. These results were explained as compressive strain reduction.

In Table 1, the FWHMs of a near band edge emission peak are 6.6 nm for sample B and 6.7 nm for sample A. It is indicated that sample B, which was grown with a Si_xN_y mask interlayer on Si substrate, has the best optical property, which is comparable to the best result achieved for GaN/Si epilayers [27–29]. The low FWHM values in our films may likely be attributed to the high-degree of crystallographic alignment of the buffer layers and to the layers without a gain structure. Wu et al. [18] used various $Al_{0.3}Ga_{0.7}N$/GaN superlattices as an intermediate layer for GaN/Si(1 1 1) epitaxial layers, in which their reported values for the FWHM values were 34.49 meV.

4. Conclusions

In summary, single-crystalline GaN films were successfully grown on Si(1 1 1) substrates using silicon nitride as the first buffer layer and as the intermediate layer by MOCVD. The thicknesses of the GaN epitaxial layers exceeded 2.2 μm. The crystalline quality and morphology of the GaN layers significantly improved after using nitride as the first buffer layer. The root-mean-square (RMS) value of the surface roughness of the GaN film grown on appropriately nitridated Si is approximately 0.8 nm as was obtained by an atomic force microscopy. When compared to the previously published results, the resultant GaN epitaxial layers exhibited the best value for the crystalline quality and morphology. Pronounced GaN (0 0 0 2), (0 0 0 4), (0 0 0 6), and two Si(1 1 1) peaks appeared in the XRD pattern. The FWHM of the double crystal X-ray rocking curve (DCXRC) for the (0 0 0 2) diffraction was 492 arcsec for sample B and 566 arcsec for sample A. These results show that there is significant improvement in the GaN crystal quality that is grown on nitridated silicon substrates. At room temperature, the PL spectrum for sample B showed that the GaN epilayer emitted light at a wavelength of 365 nm with a FWHM of 6.6 nm (33.13 meV). As a result of our investigation, it is concluded that performing the simple nitridation of silicon substrate makes it possible to grow high-quality GaN on Si by MOCVD.

Acknowledgements

This work is supported by the European Union under the projects EU-NoE-METAMORPHOSE, EU-NoE-PHOREMOST, and TUBITAK under Projects Nos. 104E090, 105E066, 105A005, and 106A017. One of the authors (E.O.) also acknowledges partial support from the Turkish Academy of Sciences.

References

[1] S. Pal, C. Jacob, Bull. Mater. Sci. 27 (2004) 501.
[2] A. Krost, A. Dadgar, Phys. Stat. Sol. (a) 194 (2002) 361.
[3] Hongbo Yu, M. Kemal Ozturk, Suleyman Ozcelik, EkmelOzbay, J. Cryst. Growth 293 (2006) 273.
[4] Hongbo Yu, Deniz Caliskan, Ekmel Ozbay, J. Appl. Phys. 100 (2006) 033501.
[5] Mutlu Gokkavas, Serkan Butun, HongBo Yu, Turgut Tut, bayram Butun, Ekmel Ozbay, Appl. Phys. Lett. 89 (2006) 143503.
[6] Serkan Butun, Mutlu Gokkavas, HongBo Yu, Ekmel Ozbay, Appl. Phys. Lett. 89 (2006) 073503.
[7] Hongbo Yu, Wlodek Strupinski, Serkan Butun, Ekmel Ozbay, Phys. Stat. Sol. (a) 203 (2006) 868.
[8] S. Zamir, B. Meyler, J. Salzman, Appl. Phys. Lett. 78 (2001) 288.

[9] S.A. Nikishin, N.N. Faleev, G. Antipov, S. Francoeur, L. Grave de Peralta, G.A. Seryogin, H. Temkin, T.I. Prokofyeva, M. Holtz, S.N.G. Chu, Appl. Phys. Lett. 75 (1999) 2073.
[10] H. Amano, M. Iwaya, N. Hayashi, T. Kashima, M. Katsuragawa, T. Takeuchi, C. Wetzel, I. Akasaki, J. Nitride Semicond. Res. 4S1 (1999) G10..
[11] Y. Kawaguchi, Y. Honda, H. Matsushima, M. Yamaguchi, K. Hiramatsu, N. Sawaki, Jpn. J. Appl. Phys. 37 (1998) L966.
[12] J.W. Yu, H.C. Lin, Z.C. Feng, L.S. Wang, S. Tripaty, S.J. Chua, Thin Solid Films 498 (2006) 108.
[13] Min-Ho Kim, Young-Gu Do, Hyon Chol Kang, Do Young Noh, Seong-Ju Park, Appl. Phys. Lett. 79 (2001) 2713.
[14] H. Ishikawa, G.Y. Zhao, N. Nakada, T. Egawa, T. Soga, T. Jimbo, M. Umeno, Phys. Stat. Sol. (a) 176 (1999) 599.
[15] A. Able, W. Wegscheider, K. Engl, J. Zweck, J. Cryst. Growth 276 (2005) 415.
[16] Wu-Yih Uena, Zhen-Yu Li, Shan-Ming Lan, Sen-Mao Liao, J. Cryst. Growth 280 (2005) 335.
[17] J. Huang, Z. Ye, L. Wang, J. Yuan, B. Zhao, H. Lu, Solid-State Electron. 46 (2002) 1231.
[18] C.-L. Wu, J.-C. Wang, M.-H. Chan, T.T. Chen, S. Gwo, Appl. Phys. Lett. 83 (2003) 4530.
[19] P.R. Hageman, S. Haffouz, V. Kirilyuk, A. Grzegorczyk, P.K. Larsen, Phys. Stat. Sol. (a) 188 (2) (2001) 523–526.
[20] Kai Cheng, M. Leys, S. Degroote, B. Van Daele, S. Boeykens, J. Derluyn, M. Germain, G. Van Tendeloo, J. Engelen, G. Borghs, J. Electron. Mater. 35 (2006) 592.
[21] S. Raghavan, J.M. Redwing, J. Cryst. Growth 261 (2004) 294.
[22] S. Raghavan, J.M. Redwing, J. Appl. Phys. 98 (2005) 023514.
[23] Seong-Hwan Jang, Cheul-Ro Lee, J. Cryst. Growth 253 (2003) 64.
[24] M.A. Mastro, C.R. Eddy Jr., D.K. Gaskill, N.D. Bassim, J. Casey, A. Rosenberg, R.T. Holm, R.L. Henry, M.E. Twigg, J. Cryst. Growth 287 (2006) 610.
[25] A. Dadgar, J. Bläsing, A. Diez, A. Alam, M. Heuken, A. Krost, Jpn. J. Appl. Phys. 39 (2000) L1183.
[26] J. Bläsing, A. Reiher, A. Dadgar, A. Diez, A. Krost, Appl. Phys. Lett. 81 (2002) 722.
[27] B.S. Zhang, M. Wu, J.P. Liu, J. Chen, J.J. Zhu, X.M. Shen, G. Feng, D.G. Zhao, Y.T. Wang, H. Yang, A.R. Boydb, J. Cryst. Growth 270 (2004) 316.
[28] P. Chen, R. Zhang, Z.M. Zhao, D.J. Xi, B. Shen, Z.Z. Chen, Y.G. Zhou, S.Y. Xie, W.F. Lu, Y.D. Zheng, J. Cryst. Growth 225 (2001) 150.
[29] I.H. Lee, S.J. Lim, Y. Park, J. Cryst. Growth 235 (2002) 73.
[30] Y.L. Tsai, J.R. Gong, J. Cryst. Growth 263 (2004) 176.
[31] M. Iwaya, T. Takeuchi, S. Yamaguchi, C. Wetzel, H. Amano, I. Akasaki, Jpn. J. Appl. Phys. 37 (1998) L316.